NASA TN D-1059

TECHNICAL NOTE

D-1059

ANALYSIS OF A PILOT-AIRPLANE LATERAL INSTABILITY EXPERIENCED WITH THE X-15 AIRPLANE

By Lawrence W. Taylor, Jr.

Flight Research Center
Edwards, Calif.

NATIONAL AERONAUTICS AND SPACE ADMINISTRATION
WASHINGTON
November 1961

NATIONAL AERONAUTICS AND SPACE ADMINISTRATION

TECHNICAL NOTE D-1059

ANALYSIS OF A PILOT-AIRPLANE LATERAL INSTABILITY EXPERIENCED WITH THE X-15 AIRPLANE

By Lawrence W. Taylor, Jr.

SUMMARY

An analysis is made of a lateral-control problem in which the pilot, through normal application of control, induces divergent oscillations in bank angle. The problem, first encountered on the X-15 simulator and later confirmed in flight, is explained through the use of root-locus plots of the pilot-airplane combination in which the pilot is represented by a human transfer function. A parameter is developed which is useful for predicting the lateral-control problem and for showing the effect of the principal aerodynamic and inertial parameters. Also, means of determining regions in the flight envelope where the pilot-airplane would be susceptible to lateral instability are developed.

The calculated lateral-control limits agree with the simulator- and flight-determined limits for the X-15 airplane.

INTRODUCTION

Airplane handling-qualities specifications have been based primarily on the response of the airplane to control inputs and on the open-loop behavior of the airplane. Open-loop considerations are not always adequate, inasmuch as some stable configurations are not controllable by the pilot. Such conditions were encountered on the X-15 flight simulator and were later confirmed in X-15 flights. Attempts to control bank angle with normal use of aileron resulted in divergent oscillations in sideslip and roll, although the airplane was stable in a stick-fixed condition. These pilot-induced oscillations should not be confused with oscillations caused by control-system lag and high airplane natural frequencies.

The closed-loop lateral control of airplanes was investigated in the study of reference 1, in which the boundary of the lateral control-lability of the human pilot was determined and a corresponding pilot transfer function was developed.

Lateral handling qualities were also studied by using a pilot-airplane system in reference 2. This study indicated that pilot-airplane instability can result if certain controlling conditions exist, even though the airplane is stable in a stick-fixed condition.

This paper considers the pilot-airplane instability encountered with the X-15 airplane. An analysis is made by utilizing the pilot transfer function of reference 1 and the methods of analysis employed in reference 2. Root-locus methods are used to indicate the effect of certain aerodynamic parameters on the stability of the pilot-airplane system. Regions in which calculations showed the pilot transfer function—airplane combination to be unstable are compared to flight conditions which were found to be uncontrollable during flight-simulator studies and in actual flight with the X-15 airplane.

SYMBOLS

b	wing span, ft
C_n	yawing-moment coefficient
$F(s)$	transfer function of the pilot
$G(s)$	transfer function of the airplane
I_X	moment of inertia about the principal X-axis, slug-ft^2
I_Z	moment of inertia about the principal Z-axis, slug-ft^2
$j\omega$	imaginary part of a root satisfying the characteristic equation
K_p	gain of the pilot
L	$\frac{\text{Rolling moment}}{I_X}$, per sec^2
M	Mach number
m	mass, slugs
N	$\frac{\text{Yawing moment}}{I_Z}$, per sec^2
p	roll rate, deg/sec or radians/sec

q	dynamic pressure, lb/sq ft
r	yaw rate, radians/sec
S	wing area, sq ft
s	Laplace transform variable
T_2	time to double amplitude of the pilot transfer function—airplane combination, sec
t	time, sec
V	velocity, ft/sec
Y	$\frac{\text{Side force}}{mV}$, per sec
α	angle of attack, deg or radians
α_0	trim angle of attack of principal axis, radians
β	angle of sideslip, deg or radians
δ_a	aileron deflection, deg or radians
ζ_φ	damping ratio of the numerator of the airplane transfer function in roll
ζ_ψ	damping ratio of short-period Dutch roll mode
σ	real part of a root satisfying the characteristic equation
τ_φ	time constant in roll, sec
φ	bank angle, deg or radians
ω_{n_φ}	undamped natural frequency of the numerator of the airplane transfer function in roll, radians/sec
ω_{n_ψ}	undamped natural frequency of short-period Dutch roll mode, radians/sec

Subscripts:

The subscripts p, r, β, δ_a, and φ indicate the partial derivative with respect to the specific subscript; that is,

$N_{\delta_a} = \frac{\partial N}{\partial \delta_a} = \frac{qSb}{I_Z} C_{n_{\delta_a}}$ which represents the yawing "moment" due to aileron deflection.

A dot above a variable indicates a derivative with respect to time; two dots denote a second derivative with respect to time.

AIRPLANE

The X-15 is a single-place rocket-powered airplane designed for flight research at high speeds and altitudes after launch from a B-52 carrier aircraft. All aerodynamic control surfaces are actuated by irreversible hydraulic systems. Longitudinal control is provided by deflection of the slab-type horizontal tail; lateral control is provided by differential deflection of the left and right portions of the horizontal tail. The movable portions of the upper and lower wedge-sectioned vertical tails provide directional control. Auxiliary damping is provided about all three axes in a conventional manner along with a "yar" damper which provides a crossfeed of the yaw-rate signal into the roll damper.

A photograph of the airplane is shown in figure 1.

ANALYSIS AND DISCUSSION

The Control Problem

During studies in which the X-15 flight simulator was used, it was learned that an important area in the flight envelope was uncontrollable without dampers. In this area the airplane appeared to the "pilot" to be dynamically unstable. The controllability of the airplane was checked at increments of 5° in angle of attack and 0.5 in Mach number. The resulting controllability boundary is presented in figure 2.

To verify the simulator results, a flight was made during which the pilot repeatedly attempted to control the X-15 without dampers at angles of attack approaching those of the controllability boundary. The angles of attack and the Mach numbers encountered in this portion of the flight are shown in figure 2. The corresponding time histories are presented in figure 3. At the higher angles of attack, the controlled airplane motion was divergent; but, at lower angles of attack the airplane was controllable. Figure 3 shows that the phasing of the pilot's control motion did not lag the airplane bank attitude,

yet the airplane oscillation increased in amplitude. The basic airplane in this region was statically and dynamically stable (fig. 4), but the pilot-airplane combination was unstable when the normal technique of controlling bank angle with aileron was used. If the rudders had also been used, the condition might have been controllable. The use of rudders in this connection is discussed in reference 1.

Human Transfer Function

H 2 2 5

The pilot has an essential role in the dynamic lateral-control problem being considered. By substituting a mathematical expression for the pilot for this control task, servomechanism theory may be used for studying the stability of the closed-loop system. During the investigation reported in reference 1, human transfer functions were developed for the pilot performing a stabilization control task near the limits of pilot controllability. The boundary of pilot control for the roll-stabilization task in terms of static directional stability and damping is shown in figure 5 (based on ref. 1). Compared are the experimentally determined controllability boundaries based on two levels of piloting experience and the controllability limit calculated by using the pilot transfer function

$$\frac{L_{\delta_a}\delta_a(s)}{\varphi(s)} = -5 - 2.9s \qquad (1)$$

This function was chosen for its simplicity and good agreement with the experimentally determined boundaries. By using this transfer function, an input for the pilot (fig. 3) was calculated for comparison with the actual control motions made by the pilot during flight. The good agreement between the pilot control motion and the motion calculated by using the human transfer function for the pilot adds validity to the use of this transfer function. The transfer function has slightly more lead than that produced by the actual pilot. It should be noted that the calculated time history was obtained by using the pilot transfer function of reference 1 and was not adjusted to match the actual pilot input. The actual transfer function of the pilot is variable, in that he adapts his control technique to the situation. The pilot transfer function discussed in this paper, therefore, is an approximation of the transfer function which best represents the pilot for the task of monitoring bank angle.

Also plotted in figure 3 is the assumed response in roll that was desired by the pilot. The difference between the actual and the desired response in roll was used with the transfer function (eq. (1)) to compute the calculated pilot input.

Root-Locus Analysis

By using a mathematical model to represent the pilot, the stability of the pilot-airplane combination can be analyzed. An efficient and descriptive method of analysis is the root-locus method (ref. 3), which shows the effect of pilot gain on the locus of roots of the system (see appendix) in the complex plane. An example of a controllable airplane is shown in figure 6(a). Note that, for the example shown, increased pilot gain causes two of the dominant roots to travel from the open-loop Dutch roll poles to the complex zeros. That these roots do not pass into the right-half plane indicates stability regardless of pilot gain.

If the relative positions of the complex poles and zeros were interchanged, as in figure 6(b), the path of the roots would loop into the right-half plane, resulting in an unstable system. Any means by which the root locus can be shifted to the left can obviate the pilot-airplane instability.

Reference 2 points out that the ratio of the distances from the origin of the zeros and poles $\frac{\omega_{n_\varphi}}{\omega_{n_\psi}}$ is significant in predicting the pilot-airplane instability. The difference between ω_{n_φ} and ω_{n_ψ} is suggested to be somewhat more useful than the ratio $\frac{\omega_{n_\varphi}}{\omega_{n_\psi}}$, inasmuch as the distance that the locus loop extends to the right is approximately proportional to $\omega_{n_\varphi} - \omega_{n_\psi}$. This difference is derived for low lateral-directional damping in the appendix as

$$\omega_{n_\varphi} - \omega_{n_\psi} \approx \frac{L_\beta \left(\alpha_0 - \frac{N_{\delta_a}}{L_{\delta_a}} \right)}{2\omega_{n_\psi}} \qquad (2)$$

Thus, large positive products of L_β and α_0, such as encountered with the X-15 airplane, or large negative products of L_β and $\frac{N_{\delta_a}}{L_{\delta_a}}$ (ref. 1) can result in pilot-airplane instability.

Effect of increased damping and directional stability.- If pilot-airplane instability is to be avoided and if $\omega_{n_\varphi} > \omega_{n_\psi}$, the loci must be reduced in size or shifted to the left. Two methods of accomplishing the shift of the pilot-airplane root locus are illustrated in figure 7(a) and figure 7(b). Figure 7(a) shows the effect of increasing the damping

in yaw $-N_r$ from 0.22 to 2.60. Since increased yaw damping translates the loci to the left, sufficient damping in yaw can prevent pilot-induced instabilities. Adverse effects of rolling moment due to rudder can nullify the improvement of a yaw damper, however, by preventing a shift to the left.

Increased roll damping can also result in a stable pilot-airplane system, but for a different reason. If only the roll-subsidence pole is changed, increased roll damping will reduce the curvature of the loci connecting the complex poles and zeros, thus increasing the damping of the pilot-airplane combination. In figure 7(b) the most important effect is the change in the damping and frequency of the Dutch roll mode. Although the additional roll damping made the airplane unstable (without pilot), it made the airplane controllable. Adverse effects can also result from large N_{δ_a} if roll dampers are used.

As was previously indicated (eq. (2)), the difference between the Dutch roll pole and zero is inversely proportional to the Dutch roll frequency. Figure 7(c) illustrates this effect by comparing the root locus for the basic flight condition to that for the directional stability N_β increased from 15.2 to 40. It is apparent that, if the Dutch roll pole and zero have approximately the same value, the root locus will describe a sector of much less radius with less possibility of crossing to the right-half plane.

Correlation of $\omega_{n_\varphi} - \omega_{n_\psi}$ With Pilot Opinion

To validate further the use of $\omega_{n_\varphi} - \omega_{n_\psi}$ as a lateral-control parameter, a flight simulator was used to investigate the controllability of the X-15 airplane at $M = 3.5$ for a wide range of $\omega_{n_\varphi} - \omega_{n_\psi}$. A rating scale (table I) similar to that presented in reference 4 was used as a guide for the four pilots who made the evaluation. The lateral control of the X-15 was rated over a range of angle of attack of 0° to 20°. Figure 8 presents the results of this evaluation as a comparison between pilot rating and the lateral-control parameter $\omega_{n_\varphi} - \omega_{n_\psi}$. In general, the pilot ratings correlate well with the parameter and follow closely the variation of the parameter with angle of attack, as shown in figure 9; for example, the pilot rating is lowest at the largest positive value of the parameter ($\alpha = 10°$).

Calculated Controllability Limit

By using the human transfer function from reference 1, the lateral controllability of the pilot-airplane combination was calculated for flight conditions from $M = 2$ to $M = 7$ (fig. 10). The controllability

limits with dampers off (neutral pilot-airplane stability or $T_2 = \infty$) are shown and, for the unstable cases, the time for the airplane motion to double amplitude is presented to indicate the severity of the lateral-control task.

The method used to obtain the contours of figure 10 is believed to be practical for the determination of the lateral stability of the pilot-airplane combination. The human transfer function (eq. (1)) indicates that the roll damping of the pilot-airplane combination is increased by the pilot such that

$$L_{p_{\text{pilot-airplane}}} = L_{p_{\text{airplane}}} - 2.9$$

H
2
2
5

In addition, a rolling moment proportional to bank angle $L_\varphi\varphi$ is added by the pilot. Additional terms also appear in the yawing-moment equation because of control coupling. The resulting equations of motion are

$$\ddot{\varphi} = L_\beta\beta + \left(L_p - 2.9\right)\dot{\varphi} - 5\varphi \tag{3}$$

$$\dot{r} = N_\beta\beta - 2.9\,\frac{N_{\delta_a}}{L_{\delta_a}}\,\dot{\varphi} - 5\,\frac{N_{\delta_\varepsilon}}{L_{\delta_\varepsilon}}\,\varphi + N_r r \tag{4}$$

$$\dot{\beta} = -r + \alpha_0 p + Y_\beta\beta \quad \text{(principal axes)} \tag{5}$$

Expansion of these equations produces the characteristic equation from which the stability of the pilot-airplane may be derived. If the problem of effective control reversal $N_\beta < l_\beta \dfrac{N_{\delta_a}}{L_{\delta_a}}$ (ref. 1) had existed, it would have been detected.

Figure 11 compares the simulator-determined lateral-control limits with the predicted lateral-control limits calculated by using the human-pilot transfer function. Also included is a segment of the control limit obtained during flight with the X-15 airplane. The correlation between these data is reasonably good; however, additional verification is needed before conclusions concerning its generality can be drawn. The fact that the pilot found uncontrollable conditions outside the computed controllability limit is consistent with the slightly greater lead indicated by the calculated pilot input in figure 3.

It should be emphasized that the controllability limits discussed apply only to the use of ailerons to control bank angle in the normal manner and do not apply to controlling with rudders normally or with ailerons using novel techniques such as those discussed in reference 1.

CONCLUDING REMARKS

The pilot-airplane lateral instability observed with the X-15 airplane was analyzed by using an experimentally developed human transfer function for the pilot and system-analysis methods. The methods used adequately explain and predict the lateral-control problem. A parameter was developed which correlates well with pilot ratings of the lateral handling qualities. The calculated area of lateral-control difficulty agreed with that determined on the X-15 piloted flight simulator and with flight data.

Flight Research Center
National Aeronautics and Space Administration
Edwards, Calif., September 1, 1961

APPENDIX

DERIVATION OF LATERAL-CONTROL PARAMETER

A parameter is derived which has a direct relationship to the level of stability of the pilot-airplane combination.

The following equations of motion of the airplane are considered to be adequate for control of bank angle

$$\left.\begin{aligned} \dot{p} &= L_p p + L_\beta \beta + L_{\delta_a}\delta_a \\ \dot{r} &= N_r r + N_\beta \beta + N_{\delta_a}\delta_a \\ \dot{\beta} &= -r + \alpha_0 p + Y_\beta \beta \end{aligned}\right\} \tag{6}$$

After applying the Laplace transformation, the equations in an array are

$$\left.\begin{array}{cccc} \beta & p & r & \delta_a \\ \hline L_\beta & (L_p - s) & 0 & L_{\delta_a} \\ N_\beta & 0 & (N_r - s) & N_{\delta_a} \\ (Y_\beta - s) & \alpha_0 & -1 & 0 \end{array}\right\} \tag{7}$$

Thus, the transfer function relating roll rate to aileron deflection is found to be

$$\frac{p(s)}{\delta_a(s)} = \frac{s\varphi(s)}{\delta_a(s)}$$

$$= \frac{L_{\delta_a}s^2 + \left(-L_{\delta_a}N_r - L_{\delta_a}Y_\beta\right)s + N_\beta L_{\delta_a} - L_\beta N_{\delta_a} + L_{\delta_a}N_r Y_\beta}{s^3 + \left(-Y_\beta - N_r - L_p\right)s^2 + \left(N_\beta - \alpha_0 L_\beta + Y_\beta N_r + Y_\beta L_p + N_r L_p\right)s - L_p N_\beta + L_\beta N_r \alpha_0 - Y_\beta N_r L_p}$$

$$= \frac{L_{\delta_a}\left(s^2 + 2\zeta_\varphi \omega_{n_\varphi} s + \omega_{n_\varphi}^2\right)}{\left(s + \frac{1}{\tau_\varphi}\right)\left(s^2 + 2\zeta_\psi \omega_{n_\psi} s + \omega_{n_\psi}^2\right)} \tag{8}$$

The pilot-airplane combination for lateral control in which only roll motions are monitored has the following block diagram

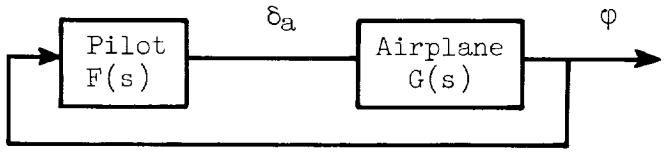

Using the human transfer function for lateral control (ref. 1), $\frac{L_{\delta_a}\delta_a(s)}{\varphi(s)} = -5 - 2.9s$, the open-loop transfer function is

$$F(s)G(s) = \frac{K_p L_{\delta_a}(1 + 0.57s)\left(s^2 + 2\zeta_\varphi \omega_{n_\varphi} s + \omega_{n_\varphi}^2\right)}{s\left(s + \frac{1}{\tau_\varphi}\right)\left(s^2 + 2\zeta_\psi \omega_{n_\psi} s + \omega_{n_\psi}^2\right)} \tag{9}$$

By using the open-loop transfer function, root-loci plots (ref. 3) can be constructed to show the change in the roots of the pilot-airplane combination as the pilot gain is increased. A typical root-locus plot in which lateral control is a problem is shown in the following sketch

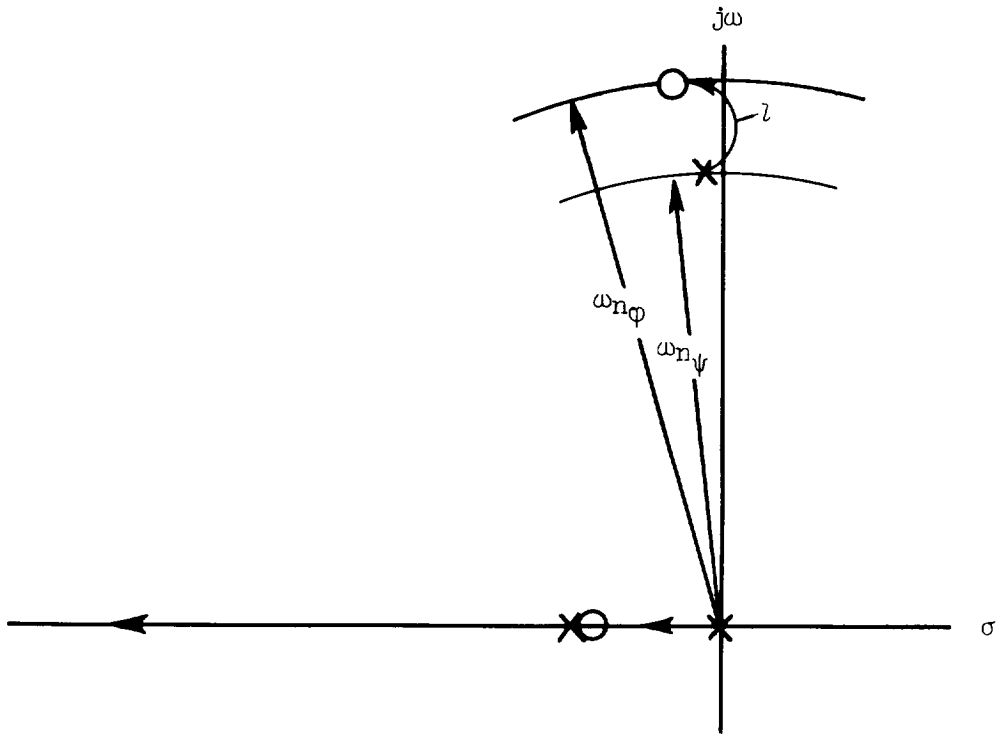

From the sketch it may be seen that a parameter which shows the distance that the loci may extend to the right indicates the severity of the pilot-airplane instability.

Consider the locus l connecting the complex pole and zero. From geometry, this locus will be a segment of a circle, inasmuch as for each point on the locus the angle between the two fixed points (the complex pole and zero) is constant. In addition, the locus will be a semicircle if the angle is near 90°, which is the case when the complex poles and zeros are sufficiently removed from the real poles and zeros (high static stability and low damping). The distance separating the complex pole and zero then equals twice the distance that the loci extend to the right from their midpoint. Thus, the distance separating the complex pole and zero is significant to the instability problem. When the real parts of the complex poles and zeros have a smaller difference than for the imaginary parts, the distance between the complex pole and zero will be approximately equal to $\omega_{n_\varphi} - \omega_{n_\psi}$. This difference, then, is suggested as a parameter which indicates the severity of the control problem.

H
2
2
5

If only low levels of damping compared to static stability are considered $\left(2\zeta_\psi\omega_{n_\psi},\ \frac{1}{\tau_\varphi},\ -N_r,\ -Y_\beta,\ -L_p \ll N_\beta,\ L_\beta,\ \omega_{n_\psi}^2\right)$, approximate expressions for ω_{n_φ} and ω_{n_ψ} can be derived from coefficients of the roll-transfer function of the airplane (eq. (8)).

By equating like coefficients in (eq. (8))

$$\omega_{n_\varphi}^2 = N_\beta - L_\beta \frac{N_{\delta_a}}{L_{\delta_a}} + N_r Y_\beta$$

$$\omega_{n_\psi}^2 + \frac{2\zeta_\psi\omega_{n_\psi}}{\tau_\varphi} = N_\beta - \alpha_0 L_\beta + Y_\beta N_r + Y_\beta L_p + N_r L_p$$

Neglecting the products of small terms

$$\omega_{n_\varphi}^2 = N_\beta - L_\beta \frac{N_{\delta_a}}{L_{\delta_a}}$$

$$\omega_{n_\psi}^2 = N_\beta - \alpha_0 L_\beta$$

it follows that

$$\omega_{n_\varphi} - \omega_{n_\psi} = \sqrt{N_\beta - L_\beta \frac{N_{\delta_a}}{L_{\delta_a}}} - \sqrt{N_\beta - \alpha_0 L_\beta}$$

$$\left(\omega_{n_\varphi} - \omega_{n_\psi} + \sqrt{N_\beta - \alpha_0 L_\beta}\right)^2 = \left(\sqrt{N_\beta - L_\beta \frac{N_{\delta_a}}{L_{\delta_a}}}\right)^2$$

$$\left(\omega_{n_\varphi} - \omega_{n_\psi}\right)^2 + 2\left(\omega_{n_\varphi} - \omega_{n_\psi}\right)\sqrt{N_\beta - \alpha_0 L_\beta} + N_\beta - \alpha_0 L_\beta = N_\beta - L_\beta \frac{N_{\delta_a}}{L_{\delta_a}}$$

if $\left(\omega_{n_\varphi} - \omega_{n_\psi}\right) \ll \omega_{n_\psi}$, ω_{n_φ} and the higher-order term is neglected

$$\omega_{n_\varphi} - \omega_{n_\psi} \approx \frac{L_\beta\left(\alpha_0 - \frac{N_{\delta_a}}{L_{\delta_a}}\right)}{2\sqrt{N_\beta - \alpha_0 L_\beta}} = \frac{L_\beta\left(\alpha_0 - \frac{N_{\delta_a}}{L_{\delta_a}}\right)}{2\omega_{n_\psi}} \tag{10}$$

Equation (10) shows clearly the effect of the key aerodynamic and inertial characteristics and is a measure of the maximum deterioration of the closed-loop Dutch roll damping.

REFERENCES

1. Taylor, Lawrence W., Jr., and Day, Richard E.: Flight Controllability Limits and Related Human Transfer Functions as Determined From Simulator and Flight Tests. NASA TN D-746, 1961.

2. Ashkenas, Irving L., and McRuer, Duane T.: The Determination of Lateral Handling Quality Requirements From Airframe-Human Pilot System Studies. WADC Tech. Rep. 59-135 (Contract No. AF 33(616)-5661), Wright Air Dev. Center, U.S. Air Force, June 1959. (Available from ASTIA as AD 212 152.)

3. Evans, Walter R.: Control-System Dynamics. McGraw-Hill Book Co., Inc., New York, 1954.

4. Cooper, George E.: Understanding and Interpreting Pilot Opinion. Aero. Eng. Rev., vol. 16, no. 3, Mar. 1957, pp. 47-51, 56.

H
2
2
5

TABLE I.- PILOT RATING SCALE[1]

General classification	Numerical rating	Handling qualities
Satisfactory	1	Easy to control precisely; little corrective control required.
	2	Good response, but necessitates attention for precise control.
	3	Acceptable controllability, but more than desired attention generally needed.
Unsatisfactory	4	Submarginal for normal use; requires excessive pilot attention.
	5	Controllability poor; demands constant pilot attention and continuous control inputs.
	6	Can be controlled, but pilot must exercise considerable care.
Unacceptable	7	Difficult to control and demands considerable pilot concentration.
	8	Controllable only with a high degree of pilot concentration and large control inputs.
	9	Extremely dangerous; can be controlled only with exceptional piloting skill.
Uncontrollable	10	Uncontrollable.

[1]Adapted from reference 4.

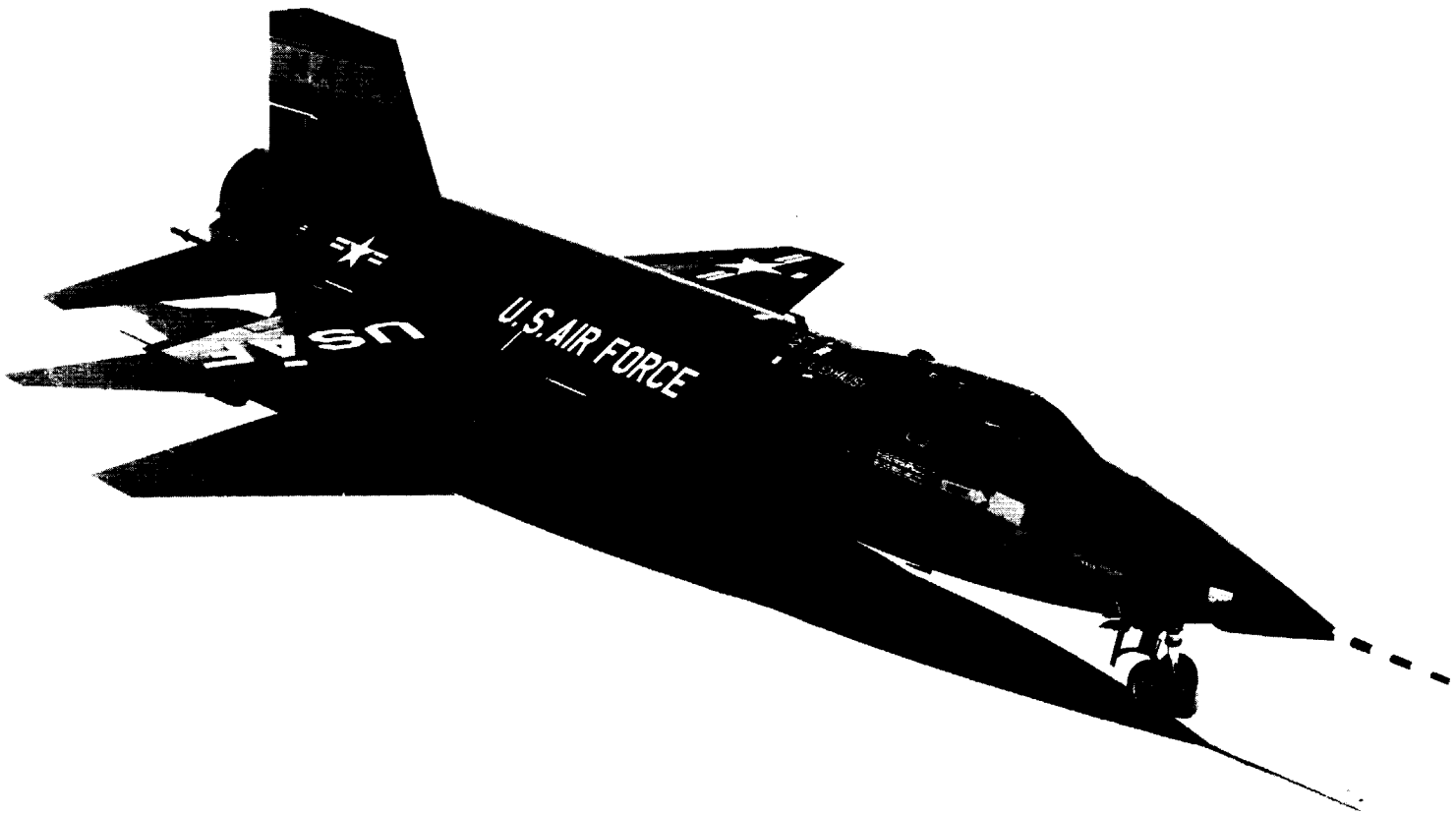

Figure 1.- Photograph of the X-15 airplane. E-5250

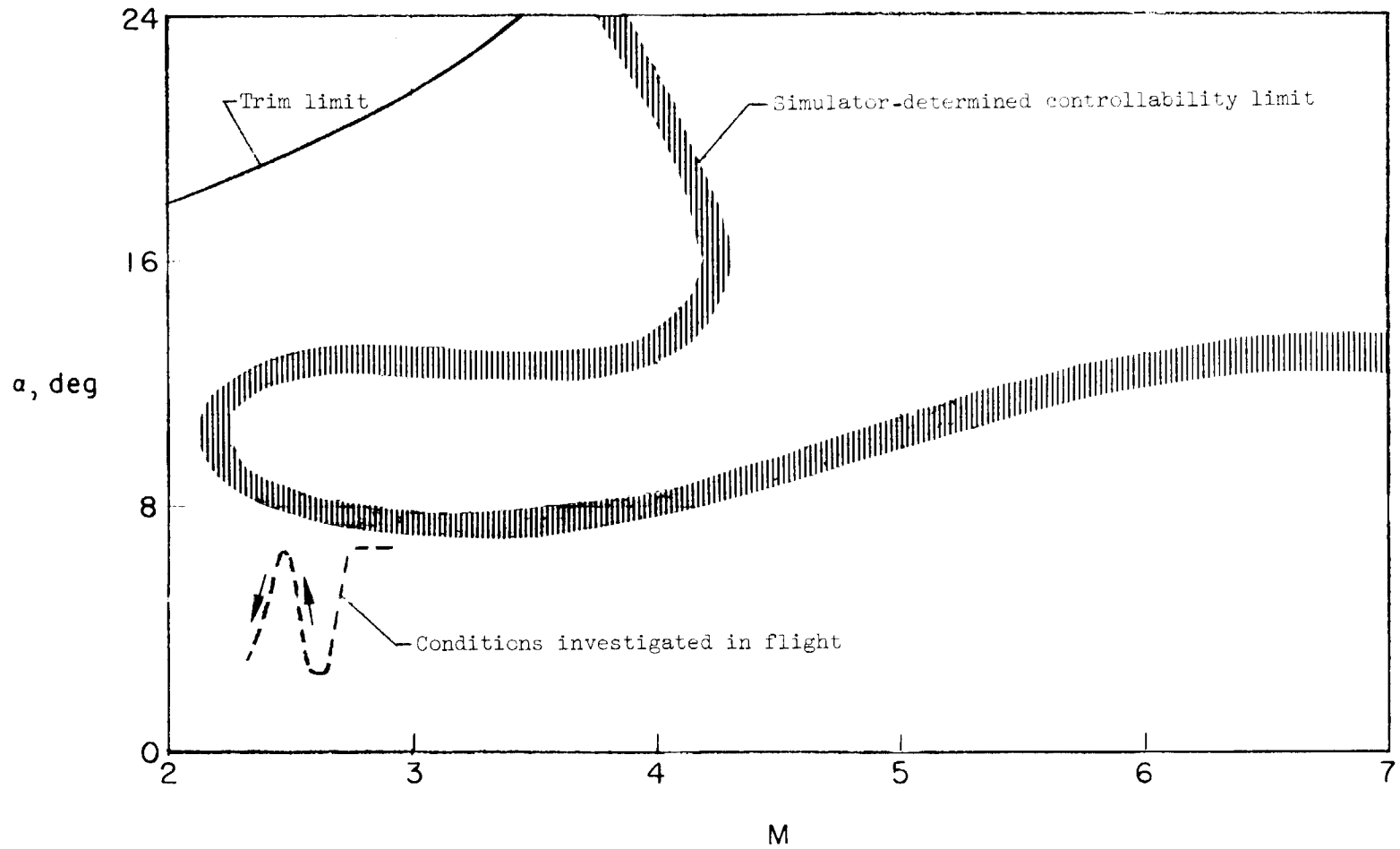

Figure 2.- Lateral-controllability limit as determined from flight-simulator studies and conditions investigated in flight.

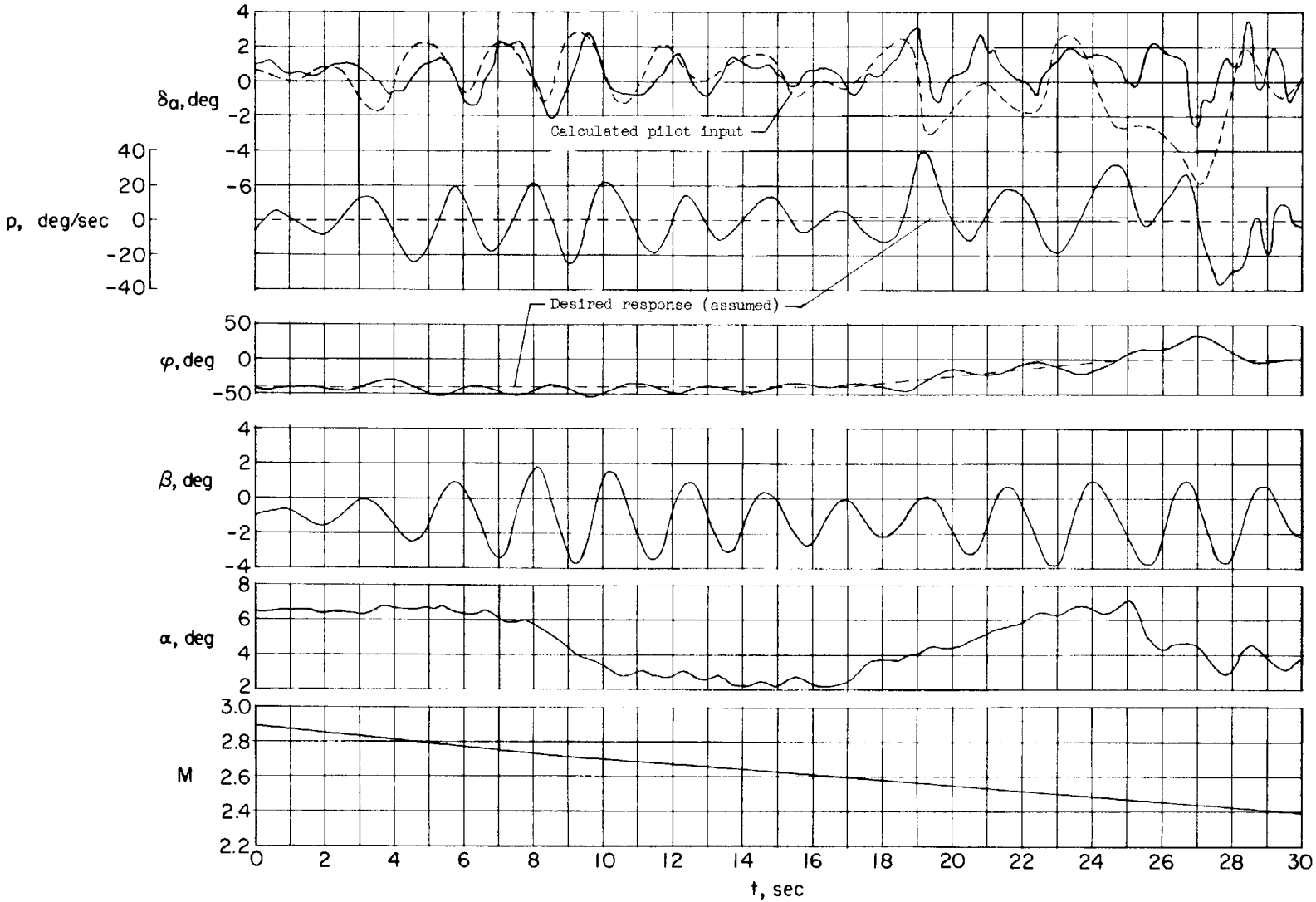

Figure 3.- Time history of an X-15 flight near the lateral-controllability limit.

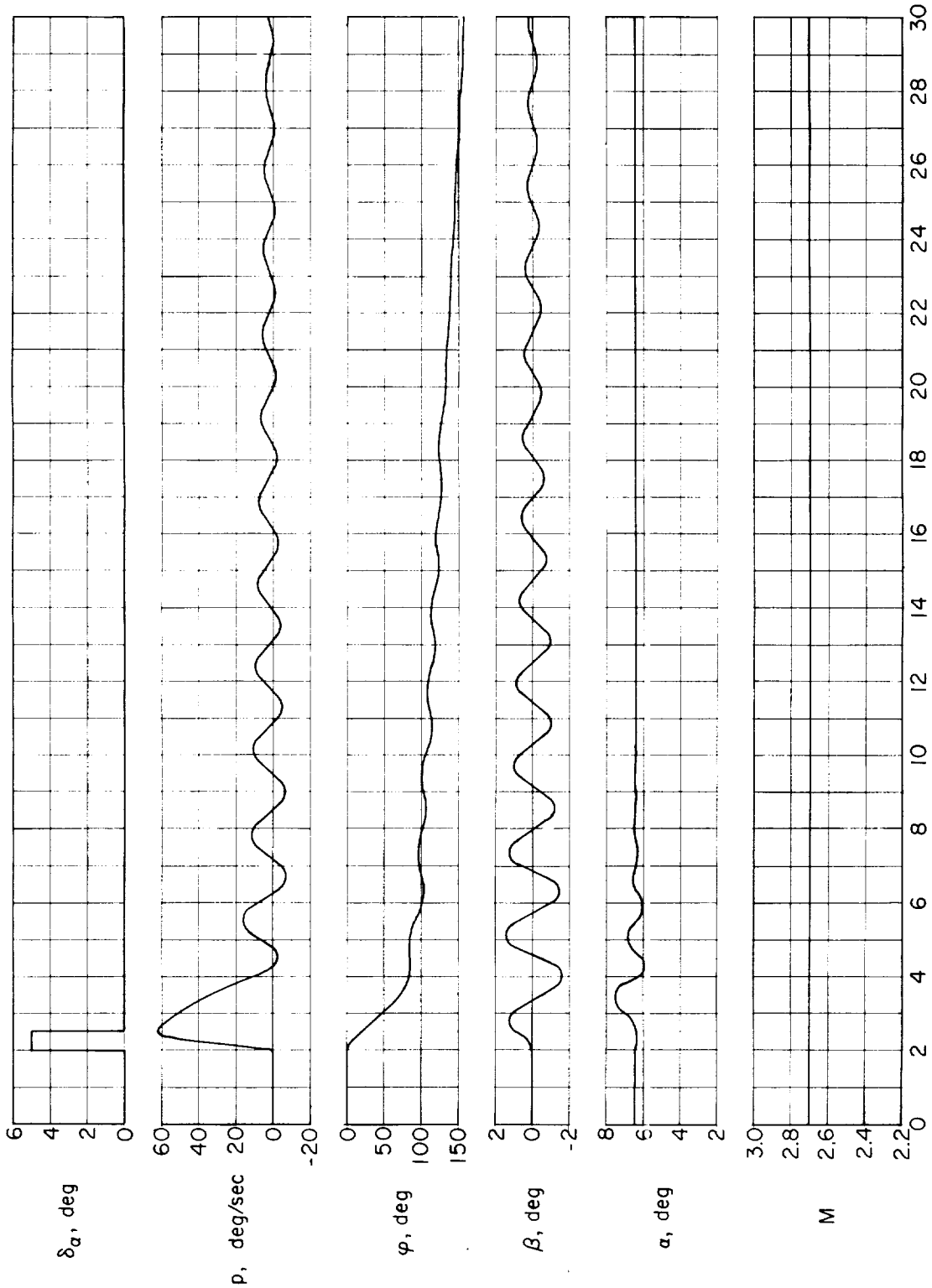

Figure 4.- X-15 airplane response to an abrupt aileron pulse.

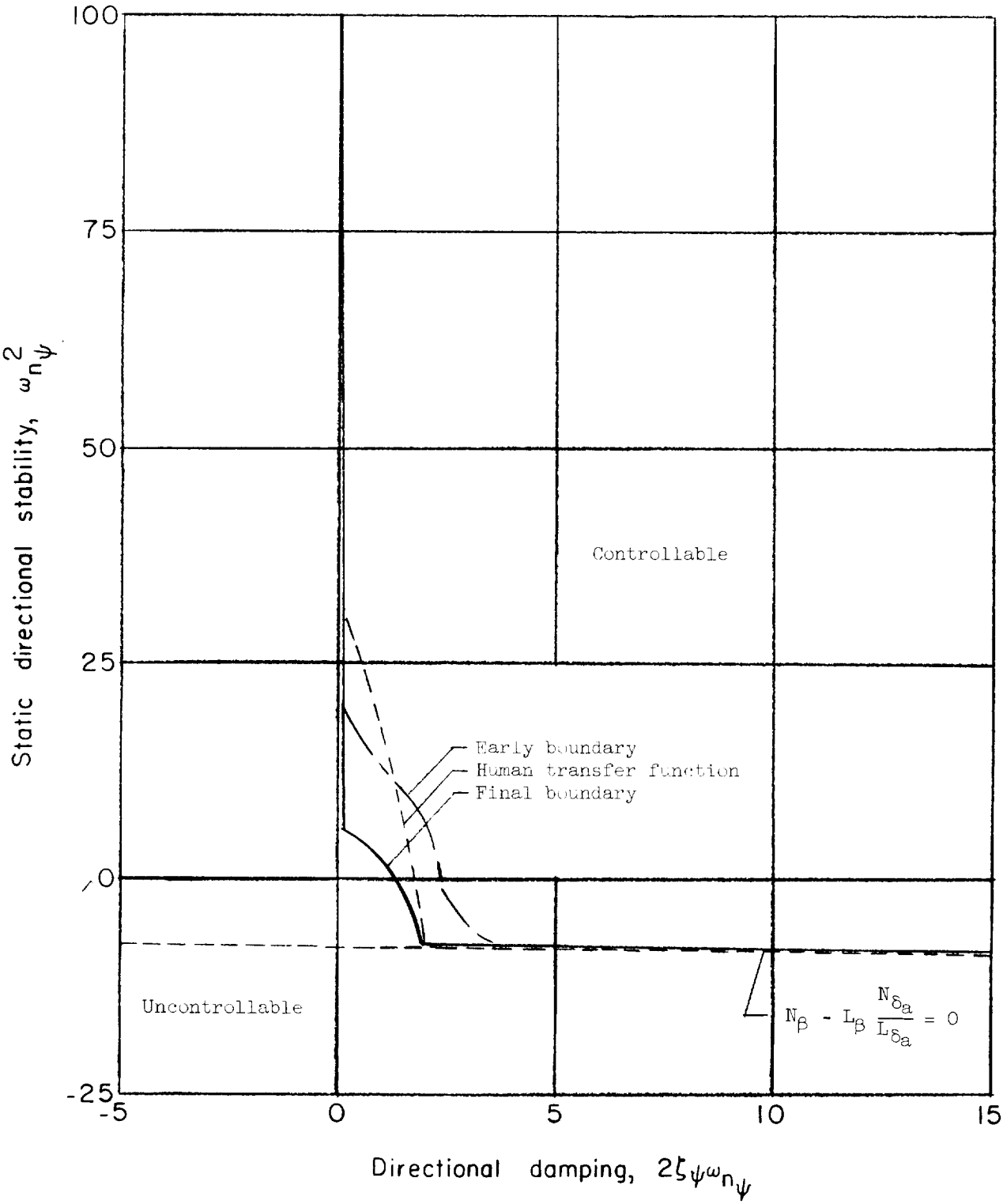

Figure 5.- Lateral-controllability limits.

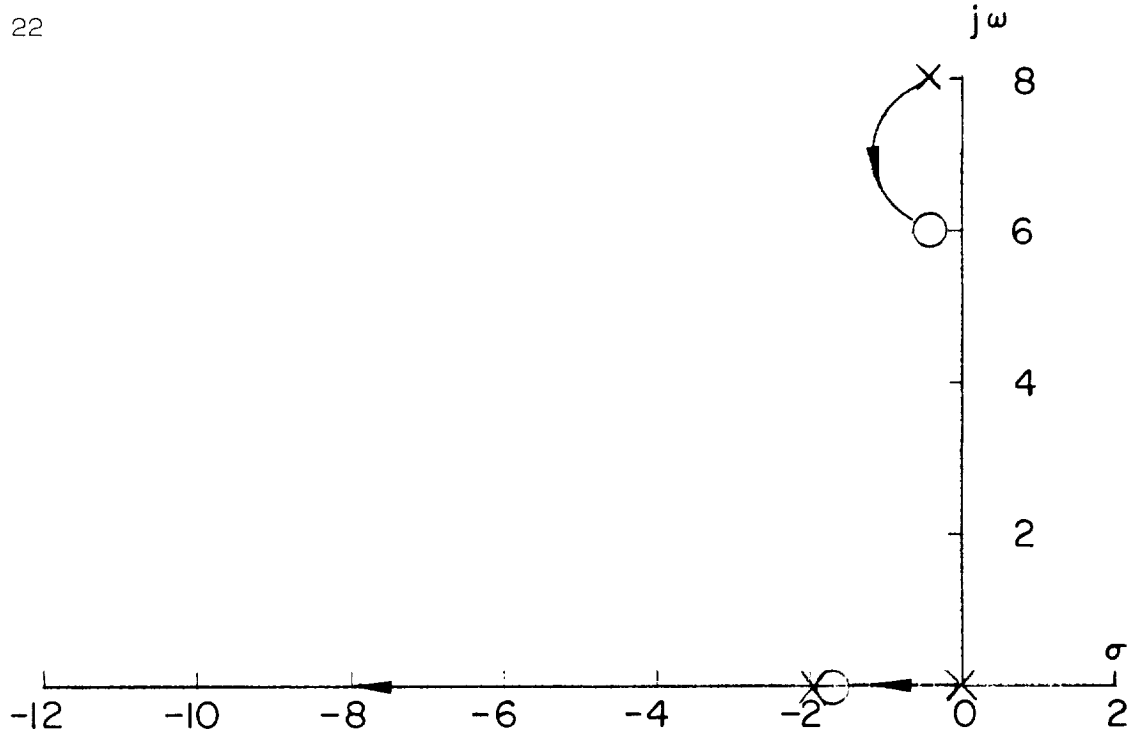

(a) $\omega_{n_\varphi} < \omega_{n_\psi}$

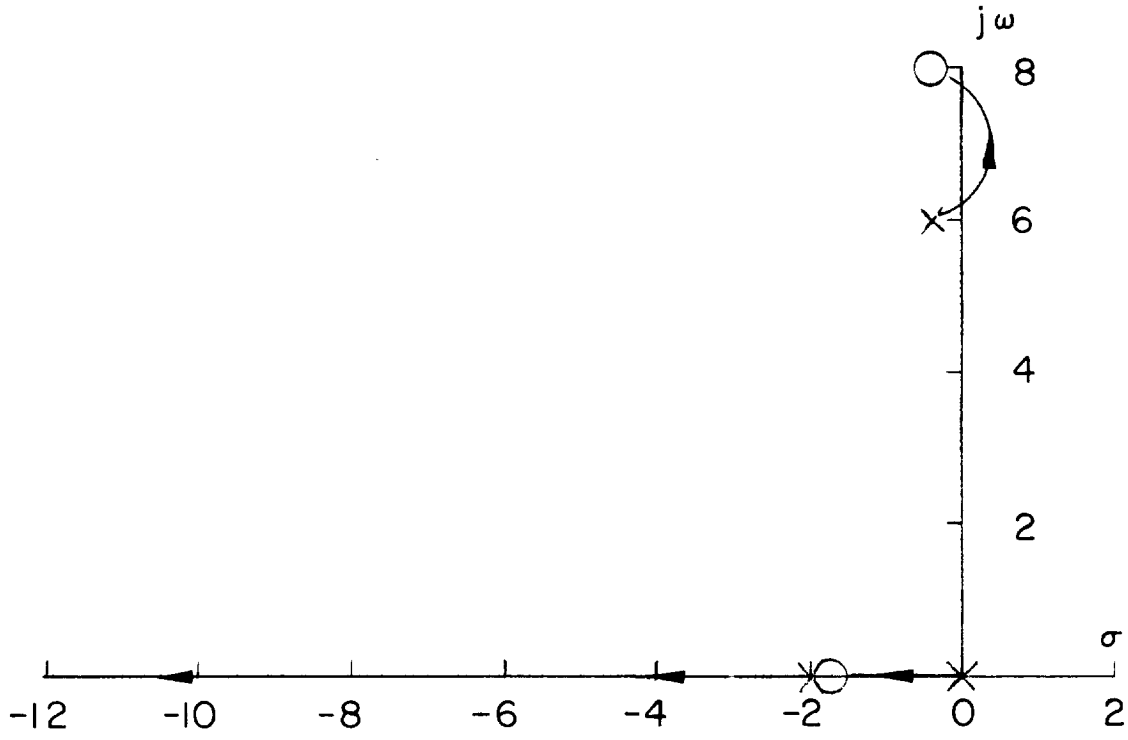

(b) $\omega_{n_\varphi} > \omega_{n_\psi}$

Figure 6.- Effect of ω_{n_φ} and ω_{n_ψ} on typical loci of the roots of the pilot-airplane combination in roll.

	Basic	Increased yaw damping
L_p	-1.0	-1.0
L_r	1.0	1.0
L_β	47	47
N_r	-0.22	-2.60
N_β	15.2	15.2
Y_β	-0.16	-0.16

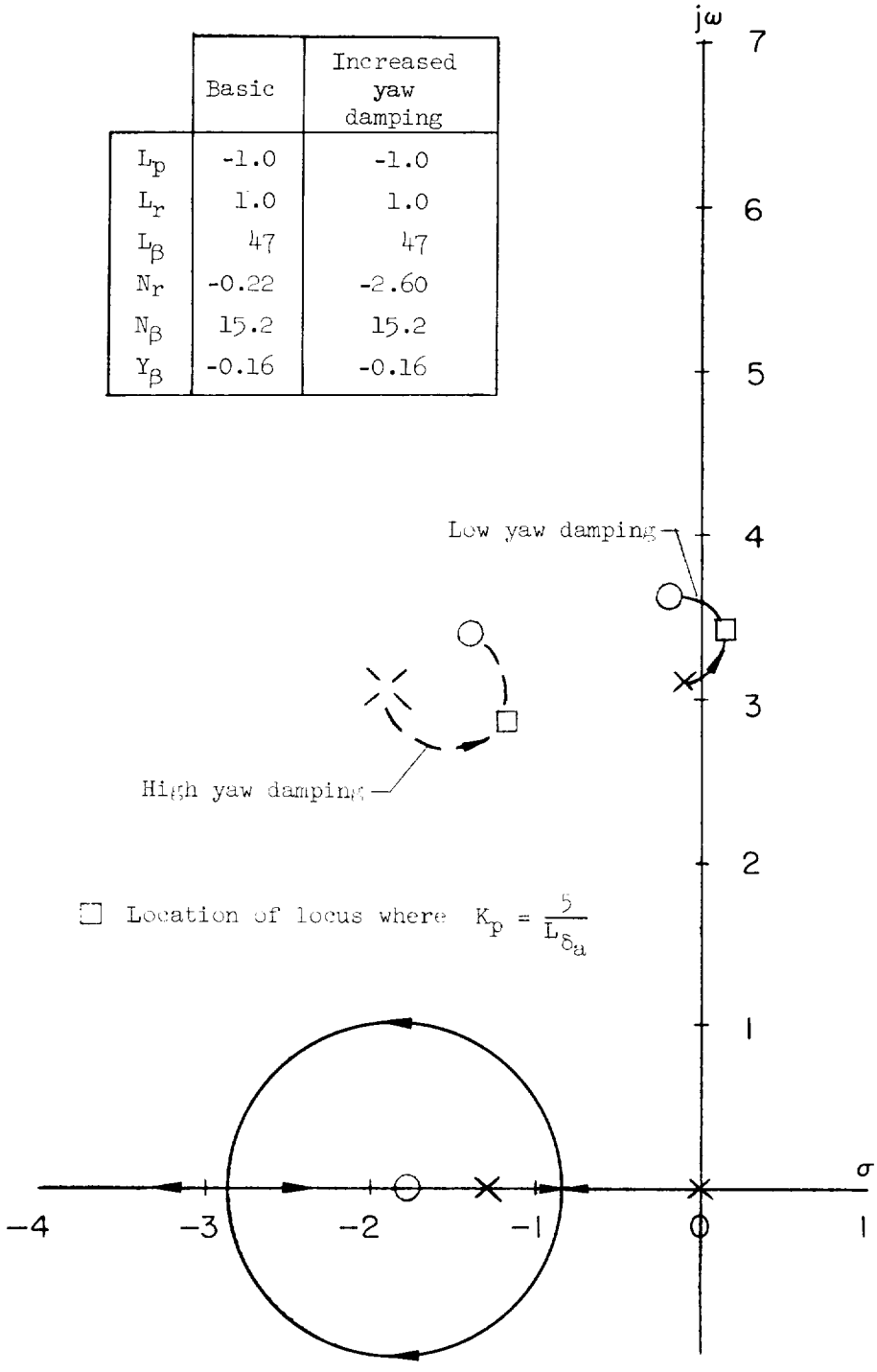

(a) Yaw damping.

Figure 7.- Effect of damping and static stability on pilot-airplane stability. M = 3.5; α_0 = 7°; q = 1,000 lb/sq ft.

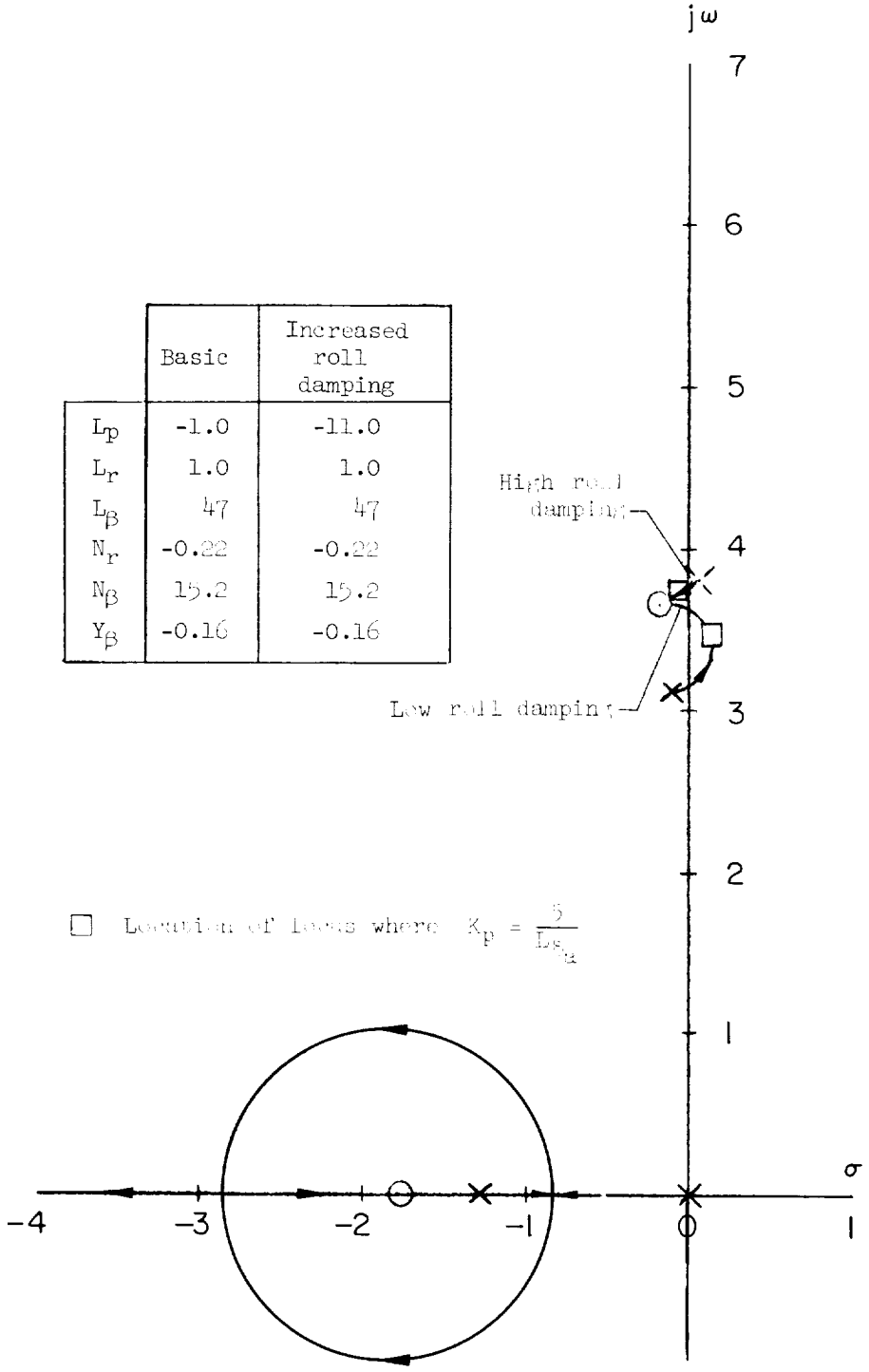

	Basic	Increased roll damping
L_p	-1.0	-11.0
L_r	1.0	1.0
L_β	47	47
N_r	-0.22	-0.22
N_β	15.2	15.2
Y_β	-0.16	-0.16

(b) Roll damping.

Figure 7.- Continued.

	Basic	Increased directional stability
L_p	-1.0	-1.0
L_r	1.0	1.0
L_β	47	47
N_r	-0.22	-0.22
N_β	15.2	40.0
Y_β	-0.16	-0.16

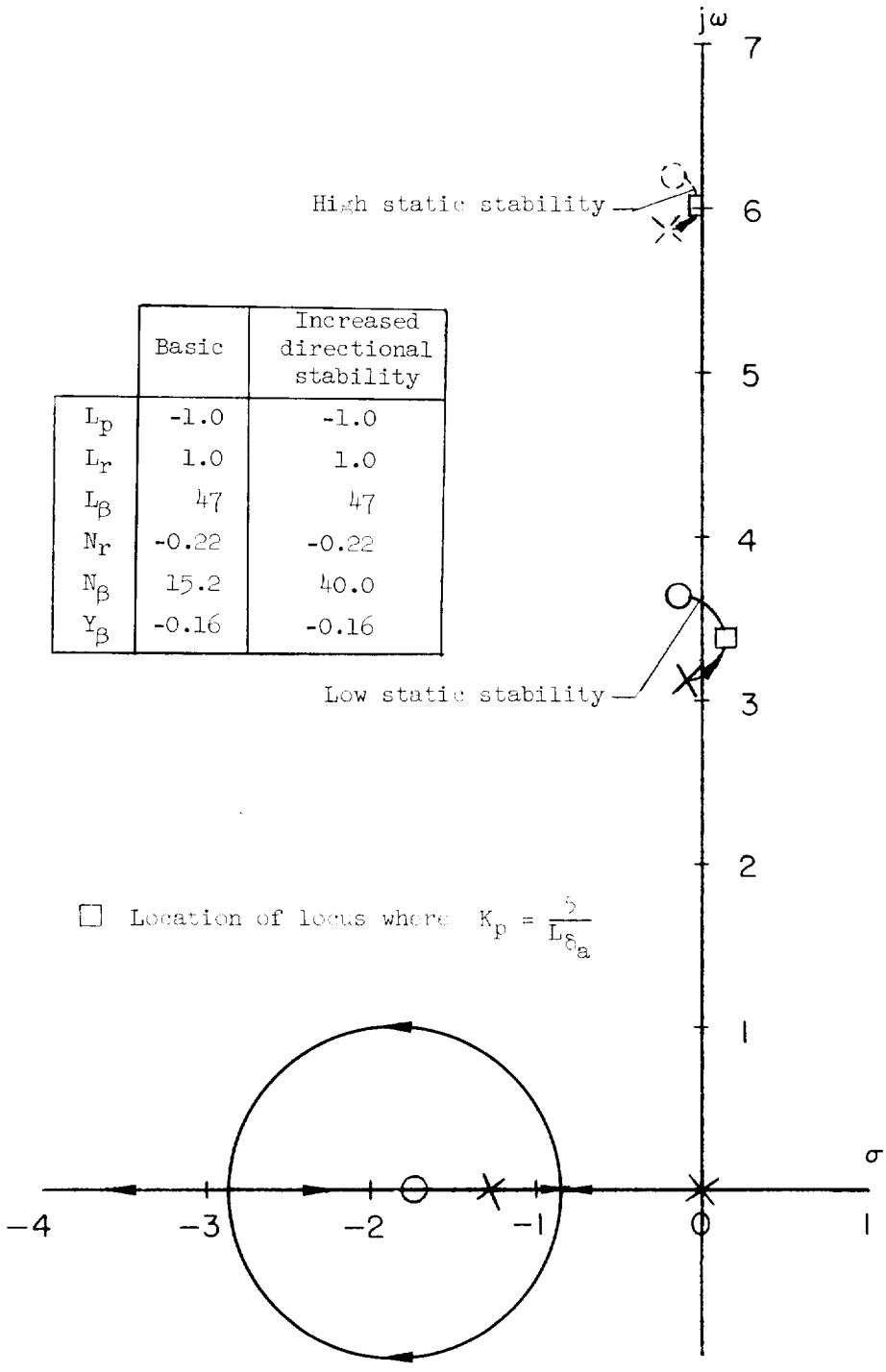

(c) Static directional stability.

Figure 7.- Concluded.

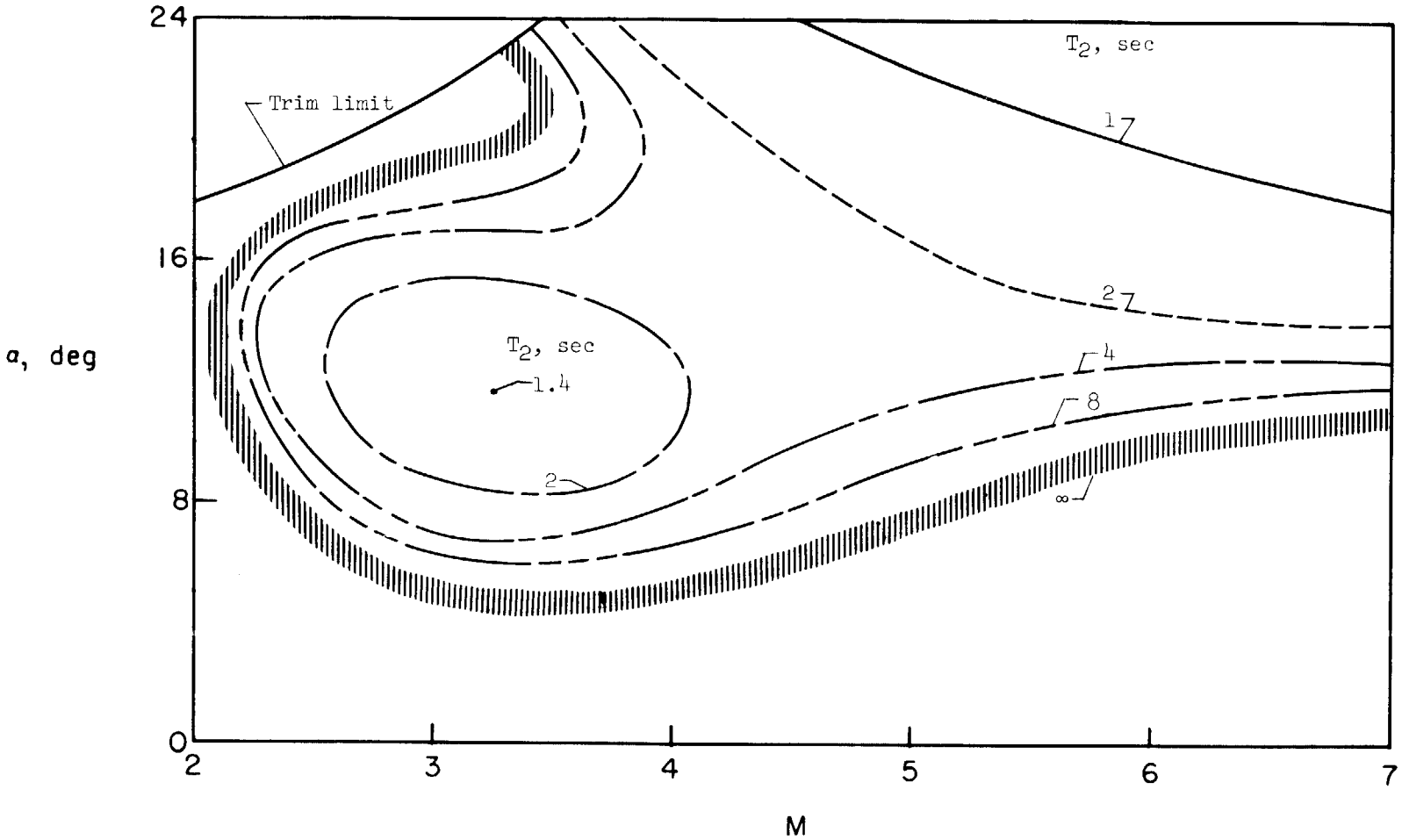

Figure 10.- Lateral-controllability contours for the basic X-15 airplane. q = 1,000 lb/sq ft.

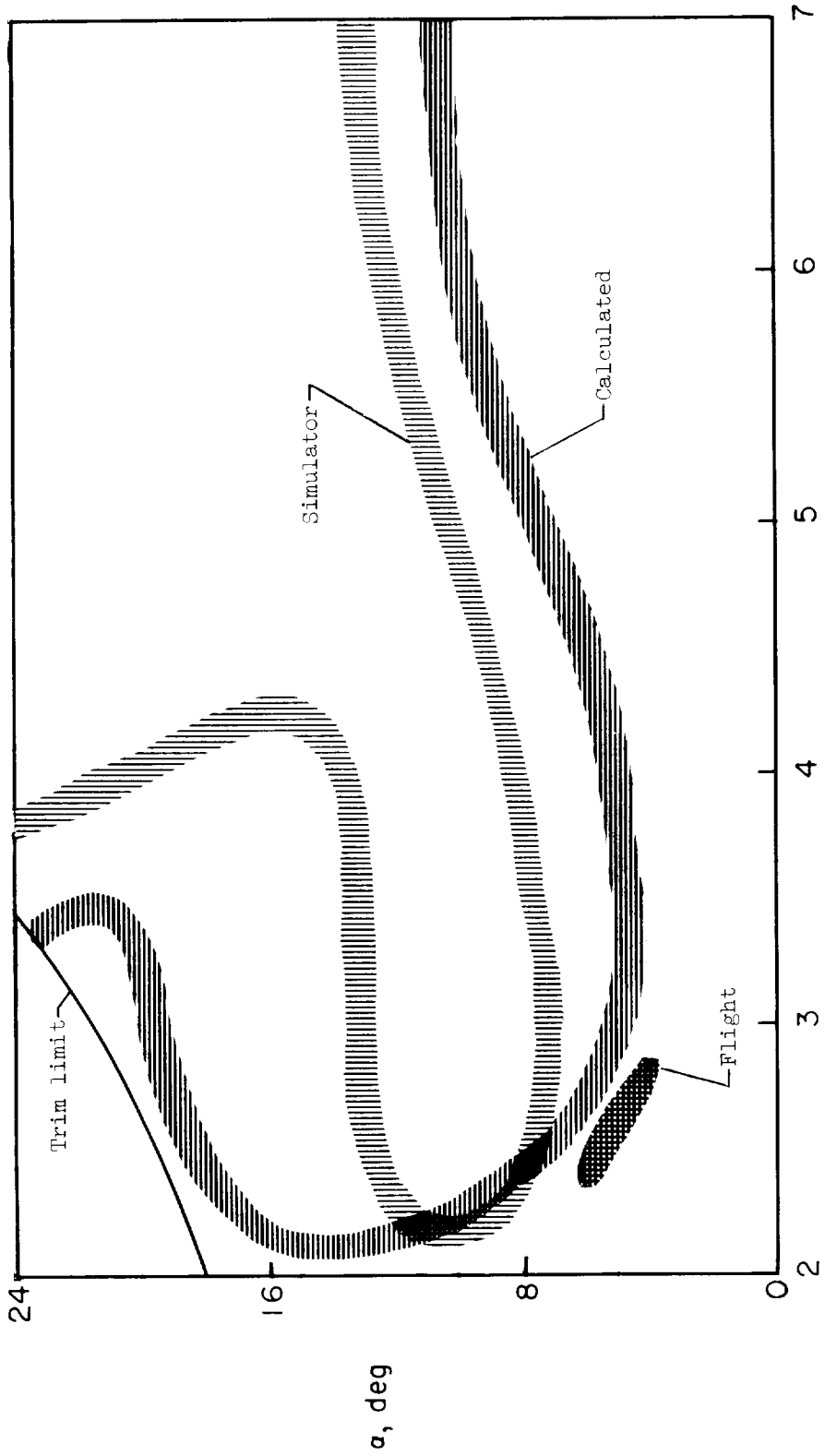

Figure 11.- Comparison of lateral-controllability limits.